Measurement of the B_d^0 lifetime in the decay mode $B_d^0 \to J/\psi(\mu^+\mu^-)K_S^0(\pi^+\pi^-)$

The DØ Collaboration
URL: http://www-d0.fnal.gov
(Dated: March 18, 2004, v1.4)

We present a preliminary measurement of the B_d^0 lifetime, using the decay mode $B_d^0 \to J/\psi(\mu^+\mu^-)K_S^0(\pi^+\pi^-)$. The data sample corresponds to an integrated luminosity of approximately 114 pb^{-1}. Using an unbinned maximum likelihood fit, we determine the B_d^0 lifetime to be $1.56^{+0.32}_{-0.25}$(stat.) $\pm$ 0.13(syst.) ps.

Preliminary Results for Winter 2004 Conferences

I. INTRODUCTION

We present a preliminary measurement of the B_d^0 lifetime in the decay mode to J/ψ K_S^0, with the J/ψ decaying to $\mu^+\mu^-$ and the K_S^0 decaying to $\pi^+\pi^-$. For this measurement we have used the dimuon data collected from October 2002 to June 2003, corresponding to an integrated luminosity of approximately 114 pb^{-1}.

To extract the B_d^0 lifetime from the data, we have used an unbinned maximum likelihood fit, fitting the mass and proper time distributions simultaneously. The background passing the B_d^0 selection cuts has been described as a combination of prompt J/ψ decays and B-meson decays producing a J/ψ. We have found it necessary to divide the B-meson background into two components; one where the K_S^0 combined with the J/ψ in the B_d^0 candidate vertex is unrelated to the B-meson decay, and one where we have a $B \to J/\psi K_S^0 X$ decay, where X is not included in the reconstruction of the B_d^0 candidate. This division was necessary due to the different mass spectra and proper time distributions of the two components of the B-meson background.

II. DATA SAMPLE

The data used was taken between October 15, 2002 and June 5, 2003, and corresponds to B-physics dimuon skim sets 1 to 21. The B-physics dimuon skim requires events to pass a L1 dimuon trigger and to contain two reconstructed muons with at least 1.5 GeV of transverse momentum. A reconstructed muon is required to have at least one track segment in at least one layer of the muon system, and this track segment must match a central track. Events containing a pair of opposite-sign muons with an invariant mass in the range of 2 to 4 GeV are selected. The selected events have been reprocessed using the "AA" tracking algorithm, with "extended" cuts for increased efficiency for high impact-parameter tracks.

Before applying our selection procedure we remove the runs marked as "bad" or "special" by the SMT, CFT and muon detector groups [1]. Runs from the range from 168618 to 169290 (except runs 169055 and 168870) were included in this analysis however, because the data from these runs suffers from a problem in the muon PDT's that does not affect this analysis. The data from run 169055 and 168870 was not used because the solenoid was off during these runs. The total luminosity in the bad runs that were removed is of the order of a few pb^{-1}.

III. EVENT SELECTION

We will now describe the selection cuts used to select J/ψ's, K_S^0's and B_d^0's. Cuts are chosen to optimize the B_d^0 signal significance $\mathcal{S} = N_S/\sqrt{N_S + N_B}$, with N_S the number of B_d^0's in the mass peak, and N_B the number of background events under the peak.

A. J/ψ selection

The J/ψ selection cuts that we have used are:

- J/ψ vertex $\chi^2 < 6$
- $p_T(J/\psi) > 3$ GeV
- p_T of each muon > 2.5 GeV
- at least 3 SMT hits on each muon

The shape used to fit the resulting mass spectrum is a double Gaussian for the J/ψ mass peak, over a linear background. The fit is shown in Fig. 1. It yields 125,000 J/ψ's in a Gaussian with a width of 59 ± 0.2 MeV, and 54,000 J/ψ's in a Gaussian with a width of 119 ± 0.5 MeV, so that the total number of J/ψ's is 183,000. The fitted J/ψ mass is 3072 ± 0.2 MeV, slightly below the PDG J/ψ mass of 3097 ± 0.04 MeV [2]. This is hypothesized to be due to not yet finalized calibration of the magnetic field and an inaccurate description of the amount of material in the detector. Ref. [3] shows that the magnetic field used in the reconstruction is approximately 0.24 % too low.

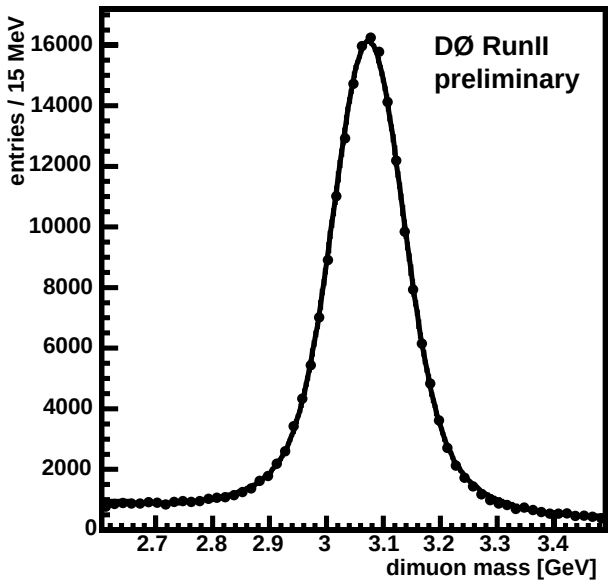

FIG. 1: Mass spectrum of two-track vertices passing J/ψ identification cuts. The fit yields a total of about 183,000 J/ψ's at a mass of 3072 ± 0.2 MeV.

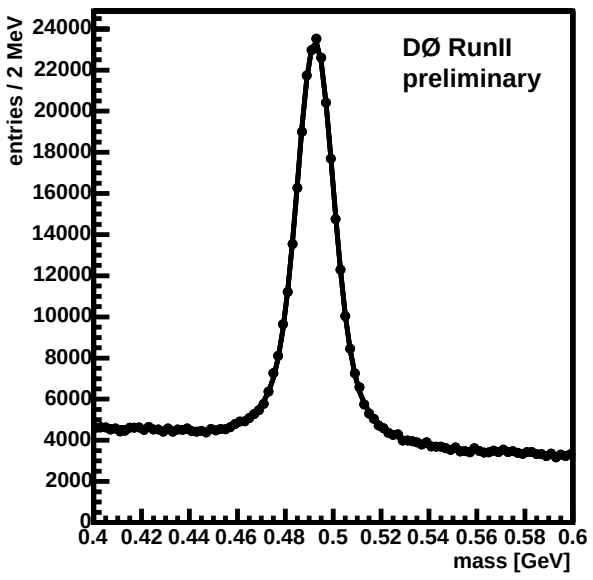

FIG. 2: Mass spectrum of two-track vertices passing K^0_S identification cuts. The fit yields a total of about 182,000 K^0_S at a mass of 493 ± 0.03 MeV.

B. K^0_S selection

Our initial K^0_S candidate sample consists of all combinations of two tracks of opposite charge, passing the following track quality cuts:

- the error on $1/p_T$ divided by $1/p_T < 0.5$
- at least 13 CFT hits on each track
- no more than 3 hits on both tracks before the vertex, and fewer than 2 misses on each track beyond the vertex

We have used the following cuts to improve signal over background:

- vertex $\chi^2 < 30$
- $p_T(K^0_S) > 0.4$ GeV
- collinearity with respect to the PV > 0

The collinearity is the cosine of the angle between the reconstructed momentum and the line connecting the PV and the secondary vertex. The range of the collinearity is from minus one to one. Our cut at zero is very loose, as not to bias the lifetime measurement at this stage.

The result of this selection is shown in Fig. 2. The background under the K^0_S peak is higher than in typical two-track mass spectra due to our very loose requirement on the collinearity. To fit the K^0_S peak in this spectrum we have used a double Gaussian. We used a straight line for the background. The first Gaussian has a width of 7 ± 0.1 MeV and contains 132,000 events. The second Gaussian has a width of 17 ± 0.8 MeV and holds 51,000 events. The total number of K^0_S's in this plot is approximately 182,000 at a mass of 493 ± 0.03 MeV, which is, as was the J/ψ mass, slightly below the PDG value.

C. B^0_d selection

The initial set of B^0_d candidates consists of all combinations of J/ψ's and K^0_S's. We applied a mass window cut on the J/ψ signal from 2.8 to 3.6 GeV, and on the K^0_S signal from 0.44 to 0.53 GeV. To reduce the number of random combinations, we apply the following addition selections:

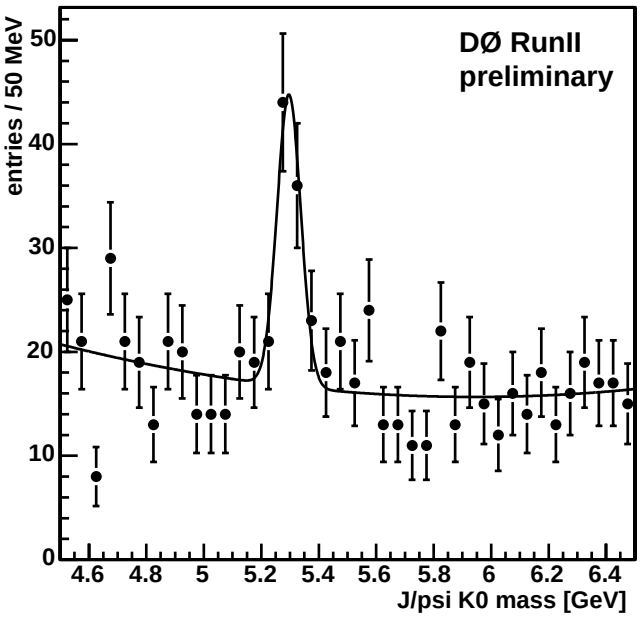

FIG. 3: Mass spectrum of $(J/\psi K_S^0)$ vertices passing all B_d^0 identification cuts. The fit yields 58 ± 20 B_d^0's over a background of 90 events, in a mass window from 5.16 to 5.43 GeV.

- χ^2 of the (J/ψ K_S^0) < 25
- χ^2 of B_d^0 "track" w.r.t. PV < 50
- $p_T(B_d^0) > 7$ GeV

To improve the p_T resolution and the vertex accuracy of the B_d^0 candidate, a mass constraint has been applied to the tracks from the J/ψ and the K_S^0. Their p_T has been corrected such that invariant mass matches the PDG value of the J/ψ and K_S^0 mass. We allow only a single B_d^0 candidate per event to contribute to the final selected event sample. In case there are multiple candidates in one event, we choose the B_d^0 candidate that has the best vertex χ^2. Finally, to be able to measure the decay length, we need a well-reconstructed primary vertex. Therefore we require at least 5 tracks attached to the PV.

The result of this selection is shown in Fig. 3. We have used a single Gaussian to fit the B_d^0 signal peak, and a parabola to fit the background. We find 58 ± 20 B_d^0's over a background of 90 events (in a mass window of 5.16-5.43 GeV). The reconstructed B_d^0 mass is 5.29 ± 0.01 GeV, with a resolution of 41 ± 11 MeV.

We also include in Fig. 4 the $(J/\psi K_S^0)$ mass spectrum from a signal MC sample containing 77,000 events. To properly fit the mass peak, a double Gaussian is needed. The first Gaussian holds 69 ± 7 % of the events, and has a width of 39 ± 3 MeV. The second Gaussian has a width of 10 ± 2 MeV.

IV. B_d^0 PROPER TIME MEASUREMENT

In this section the reconstruction of the proper time of B_d^0 mesons will be described. The measurement strategy is to reconstruct the transverse decay length L_{xy} of the B_d^0 (the component of the decay length in the plane perpendicular to the beam axis), and its p_T. The proper time $c\tau(B_d^0)$ will be calculated using the relation:

$$c\tau(B_d^0) = \frac{L_{xyz}}{\beta\gamma} = \frac{L_{xy}}{p_T} \cdot m_{B_d^0} \tag{1}$$

The $c\tau$ distribution follows an exponential distribution, and the B_d^0 lifetime is the time constant of this distribution. For the mass of the B_d^0 we will use the PDG 2002 value [2]. The following sections will discuss the measurement of the B_d^0 decay length and the determination of the p_T of the B_d^0.

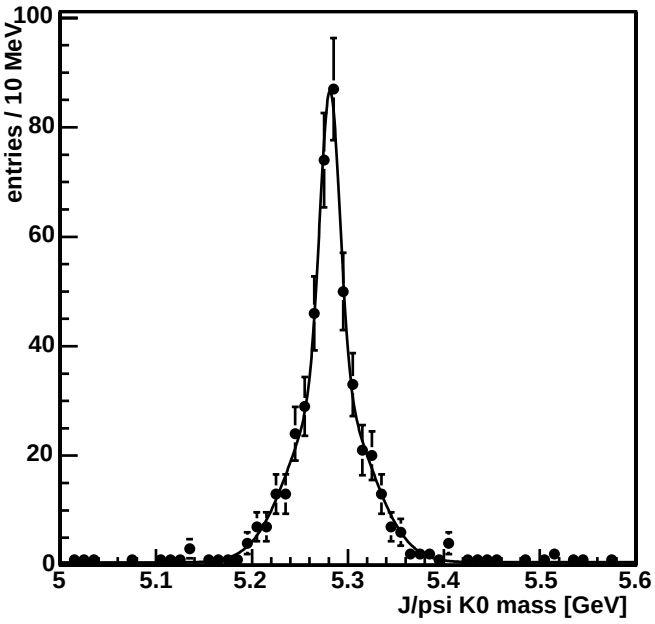

FIG. 4: Mass spectrum of $(J/\psi K_S^0)$ vertices passing all B_d^0 identification cuts in a signal MC sample.

A. Decay length measurement

The decay length of the B_d^0 mesons is primarily measured from the position of their production and decay vertices. The production vertex is assumed to be the reconstructed primary vertex.

We have studied the accuracy on our determination of the PV on Monte Carlo data by comparing the reconstructed PV to the PV as it is known from the generator information (the MC true PV). Fig. 5 shows the distribution of the residuals in the direction of flight of the B_d^0 (labeled ΔL), and the residual in the coordinate transverse to this direction (labeled ΔT). The definition of ΔL and ΔT is illustrated in Fig. 6.

To fit the distributions in Fig. 5, we have used a fit function consisting of two Gaussians with different width but identical means:

$$f(x) = C \cdot \left(\frac{\alpha}{\sigma_1\sqrt{2\pi}} \cdot \mathrm{e}^{-\frac{(x-\mu)^2}{2\sigma_1^2}} + \frac{1-\alpha}{\sigma_2\sqrt{2\pi}} \cdot \mathrm{e}^{-\frac{(x-\mu)^2}{2\sigma_2^2}} \right) \tag{2}$$

The standard deviation of this function is $\sigma = \sqrt{\alpha\sigma_1^2 + (1-\alpha)\sigma_2^2}$. In Table I we have listed the standard deviation from the fits for the different distributions. For reference we have also included the fit results from the distribution in Cartesian coordinates.

We have followed the same procedure to study the position accuracy on our determination of the B_d^0 decay vertex. The results are shown in Fig. 7 and Table II.

The flight direction is much more accurately determined by the reconstructed momentum vector, than by the line connecting the PV and reconstructed B vertex, especially at shorter decay lengths. This is the reason our decay length determination improves if we project the decay length vector on the momentum vector. This is comparable to using only the L component of the decay length vector (see Fig. 6). We say "comparable", because the L direction is defined by the MC true momentum, and we project on the reconstructed momentum.

B. Determination of $p_T(B_d^0)$

The measurement of the p_T of the B_d^0's relies on the result of the vertex fits of the J/ψ and the K_S^0. In fitting the J/ψ and K_S^0 vertices, a mass constraint is applied, which results in an improved momentum determination, both in terms of direction and p_T. The p_T of the B_d^0 is simply the sum of the J/ψ and K_S^0 momenta.

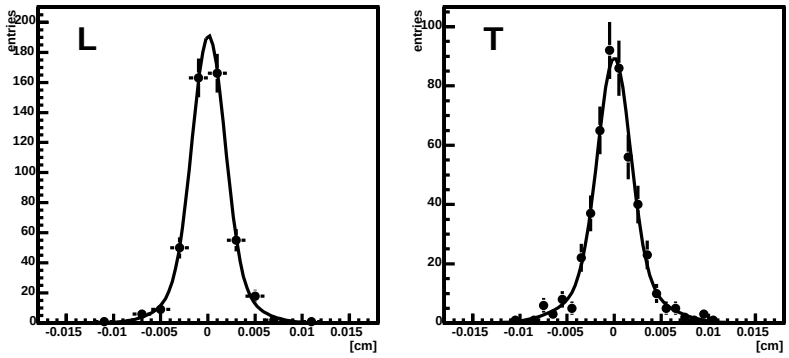

FIG. 5: Distance from reconstructed PV to the MC true PV in L and T coordinates (see Fig. 6). See Table I for the results of the fits.

Coordinate	mean $[\mu m]$	std.dev. $[\mu m]$	σ_1 $[\mu m]$	σ_2 $[\mu m]$	α
x	0.7 ± 1.02	25.7 ± 1.79	13.2 ± 1.94	33.1 ± 2.54	0.47
y	1.5 ± 0.92	24.6 ± 2.24	14.5 ± 1.76	38.2 ± 4.33	0.68
z	1.6 ± 1.69	54.0 ± 5.42	27.5 ± 2.77	107.3 ± 13.29	0.80
L	0.8 ± 0.99	23.4 ± 2.18	17.0 ± 1.74	36.1 ± 5.00	0.75
T	0.0 ± 1.07	27.1 ± 2.13	17.2 ± 1.49	41.2 ± 4.24	0.69

TABLE I: Standard deviation of PV residual distributions, in different coordinates.

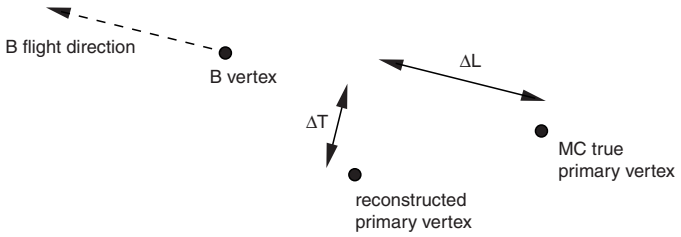

FIG. 6: The definition of ΔT and ΔL, as used in describing the vertexing resolution.

In Monte Carlo data we can compare the p_T measured to the actual, MC true p_T. The distribution of the difference is shown in Fig. 8. To estimate the resolution, we have fit a Gaussian distribution, although technically the error of $1/p_T$ is expected to follow a Gaussian distribution, and the error on p_T therefore is not. This fit yields a standard deviation of 49 ± 4 MeV. The mean is consistent with zero.

V. B_d^0 LIFETIME MEASUREMENT USING A TWO-DIMENSIONAL FIT

We determine the B_d^0 lifetime using a two-dimensional unbinned maximum likelihood fit. This procedure defines a likelihood function. Given a set of fit parameters, this likelihood function yields the likelihood that a set of events follows a distribution (the fit shape). The fit parameters maximizing the likelihood function are the fit result.

The likelihood function is given by:

$$\mathcal{L} = \prod_{i=1}^{N} \left[\alpha f^i_{sig}\left(m_i, (c\tau)_i, \sigma(c\tau)_i\right) + (1-\alpha) f^i_{bkg}(m_i, (c\tau)_i, \sigma(c\tau)_i) \right] \tag{3}$$

Where α is the fraction of signal events in the candidate sample. The index i runs from 1 to the number of B_d^0 candidates N. f^i_{sig} and f^i_{bkg} are probability density functions (PDF's) for signal and background respectively, as a function of the reconstructed mass m_i and proper time $(c\tau)_i$ (with error $\sigma(c\tau)_i$) of each candidate.

The PDF for background is the sum of two contributions, a prompt J/ψ and a long-lived contribution:

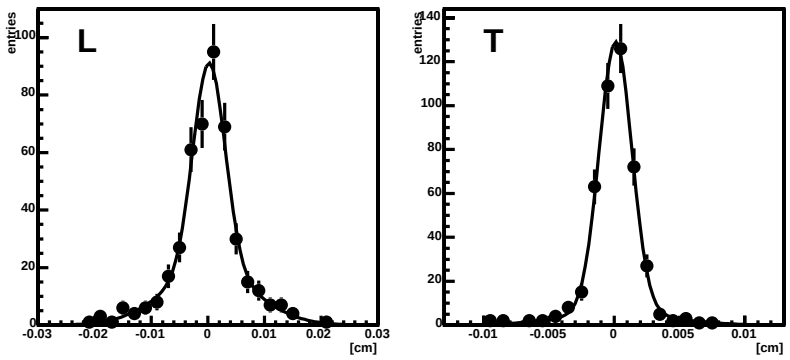

FIG. 7: Distance from reconstructed B decay vertex to MC true B decay vertex in L and T coordinates (see Fig. 6). See Table II for the results of the fits.

Coordinate	mean $[\mu m]$	std.dev. $[\mu m]$	σ_1 $[\mu m]$	σ_2 $[\mu m]$	α
x	-0.8 ± 1.45	41.1 ± 3.21	21.9 ± 1.81	68.7 ± 6.57	0.72
y	-3.2 ± 1.40	42.4 ± 3.10	19.6 ± 2.02	64.8 ± 5.39	0.63
z	1.9 ± 3.03	95.7 ± 7.70	49.9 ± 3.36	181.2 ± 18.21	0.78
L	2.2 ± 2.07	55.9 ± 3.84	28.4 ± 2.75	79.8 ± 6.29	0.58
T	1.1 ± 0.68	18.8 ± 1.59	12.5 ± 0.64	41.0 ± 5.49	0.87

TABLE II: Standard deviation of B vertex residual distributions, in different coordinates.

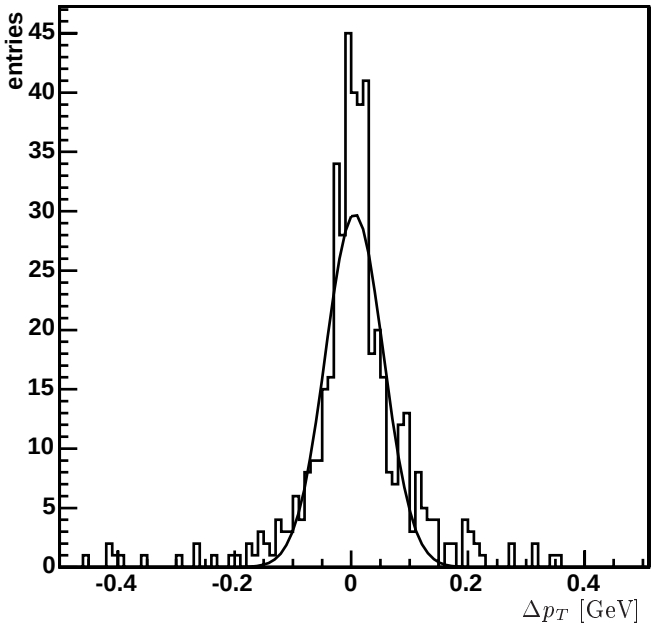

FIG. 8: The difference between reconstructed p_T and MC true p_T of a B_d^0 in a $B_d^0 \to J/\psi K_S^0$ MC sample.

$$f_{bkg}^i(m_i, (c\tau)_i, \sigma(c\tau)_i) = \alpha_{prompt} \cdot f_{prompt} + (1 - \alpha_{prompt}) \cdot f_{LL} \tag{4}$$

The prompt contribution can be factorized into a separate time and mass factor: $f_{prompt} = f_{prompt}^{time} \cdot f_{prompt}^{mass}$. The characteristics of the long-lived component f_{LL} will be discussed later.

We will use a uniform distribution to describe the mass distribution of prompt J/ψ decays, because we have shown this to be a good approximation using a sample of prompt J/ψ Monte Carlo events. As the proper time distribution of prompt J/ψ decays, we use a double Gaussian:

$$f^{time}_{prompt} = \frac{1-\alpha_2}{F_{c\tau,1}\cdot\sigma(c\tau)_i\sqrt{2\pi}}\cdot\exp\left(-\frac{1}{2}\left(\frac{(c\tau)_i}{F_{c\tau,1}\cdot\sigma(c\tau)_i}\right)^2\right) + \frac{\alpha_2}{F_{c\tau,2}\cdot\sigma(c\tau)_i\sqrt{2\pi}}\cdot\exp\left(-\frac{1}{2}\left(\frac{(c\tau)_i}{F_{c\tau,2}\cdot\sigma(c\tau)_i}\right)^2\right) \quad (5)$$

Here $F_{c\tau,1}$ and $F_{c\tau,2}$ are scale factors to the error $\sigma(c\tau)_i$ from the vertex fit. The standard deviation of the function f^{time}_{prompt} is $\sigma_{weighted}$ and given by

$$\sigma_{weighted} = \sqrt{(1-\alpha_2)(F_{c\tau,1}\cdot\sigma(c\tau)_i)^2 + \alpha_2(F_{c\tau,2}\cdot\sigma(c\tau)_i)^2} \quad (6)$$

The long-lived contribution is composed of two components. Both of these consist of J/ψ's from B-decays. In the first contribution, which we label "unrelated K^0_S", the K^0_S that is used to form the (J/ψ K^0_S) vertex is not related to the B-decay. Usually this means the K^0_S originated from the PV, or that it has been misidentified. In the events from the other long-lived contribution, labeled "missing decay products", both the J/ψ and the K^0_S are from the same B-decay, but the B-decay in question was not a $B^0_d \to J/\psi K^0_S$ decay. In these decays there have been additional B-decay products, that were not identified by our reconstruction. For both the "unrelated K^0_S" contribution and the "missing decay products" we will now define a proper time and a mass PDF.

The proper time distributions of both contributions follow an exponential convoluted with a Gaussian. The width of the Gaussian in both cases is the $\sigma_{weighted}$ defined in Eqn. 6. The difference is in the slope of the exponentials. For the missing decay products the slope is of the order of the lifetime of B-mesons (which differ by no more than 20%). We expect to obtain a somewhat higher value though, due to the underestimation of the p_T of the reconstructed B (as we didn't account for all decay products). The lifetime of the "unrelated K^0_S" contribution is significantly shorter. This is due to decreasing efficiency for larger decay lengths, as well as a bias toward shorter decay lengths. Remember that in these events, the J/ψ comes from a B-decay and the K^0_S generally comes from the PV. The combination of the K^0_S and the J/ψ in a single vertex will bias the decay length toward smaller values. Additionally, for larger decay lengths, the χ^2 of the vertex will increase, resulting in a larger chance for this vertex to be removed from the sample by our selection cuts.

The shape of the mass distribution for the "missing decay products" contribution is best approximated using a (J/ψ K^0_S) mass distribution. To obtain a histogram with reasonable statistics, we form a (J/ψ K^0_S) mass spectrum from the generator information from a $B \to J/\psi X$ sample, and smear it using the J/ψ and K^0_S mass resolutions we obtained from data. The resulting histogram is shown in Fig. 9 (b). The mass distribution of the "unrelated K^0_S's" has been studied in a Monte Carlo sample and found to be compatible with a uniform distribution.

The long-lived contribution f_{LL}, defined in Eqn. 4, is given by:

$$f_{LL} = (1-\alpha_{unrel.K^0})(f^{time}_{miss}\cdot f^{mass}_{miss}) + \alpha_{unrel.K^0}(f^{time}_{unrel.K^0}\cdot f^{mass}_{unrel.K^0}) \quad (7)$$

A graphical representation of the PDF's, associated with the long-lived contributions, is given in Fig. 9.

The PDF for signal is the product of the mass and time PDF's for signal: $f_{sig} = f^{mass}_{sig}\cdot f^{time}_{sig}$. As the mass PDF for signal f^{mass}_{sig}, we use a double Gaussian with mean $m_{B^0_d}$ (fixed to the PDG value), standard deviations $\sigma_{m,1}$ and $\sigma_{m,2}$ and weight of the second Gaussian $\alpha_{B,2}$. The reason for using a double Gaussian, is that a single Gaussian for the mass peak in the final two-dimensional fit does not have a stable minimum for the width. Comparing to the double Gaussian that was necessary to fit the mass peak in signal MC, it appears that the fit in data either chooses to fit the single Gaussian to all B^0_d candidates, or it chooses to fit the peak to the candidates in the narrow Gaussian only. If we use a double Gaussian, we find a stable result for the different parameters of the mass peak.

The proper time PDF for signal f^{time}_{sig} is an exponential convoluted with a Gaussian. The slope of the exponential is the B^0_d lifetime $\lambda(B^0_d)$. The width of the Gaussian is the weighted error on the $c\tau$ measurement $\sigma_{weighted}$, as defined earlier. An overview of the PDF's used to describe the signal and prompt J/ψ contributions is given in Fig. 10.

The parameters, necessary to describe all PDF's that we have defined are:

- the signal fraction α, the fraction of all background that is prompt J/ψ α_{prompt}, and the fraction of long-lived background that is "unrelated K^0_S" $\alpha_{unrel.K}$,
- the B^0_d mass $m_{B^0_d}$, widths $\sigma_{m,1}$ and $\sigma_{m,2}$ and relative weight $\alpha_{B,2}$,

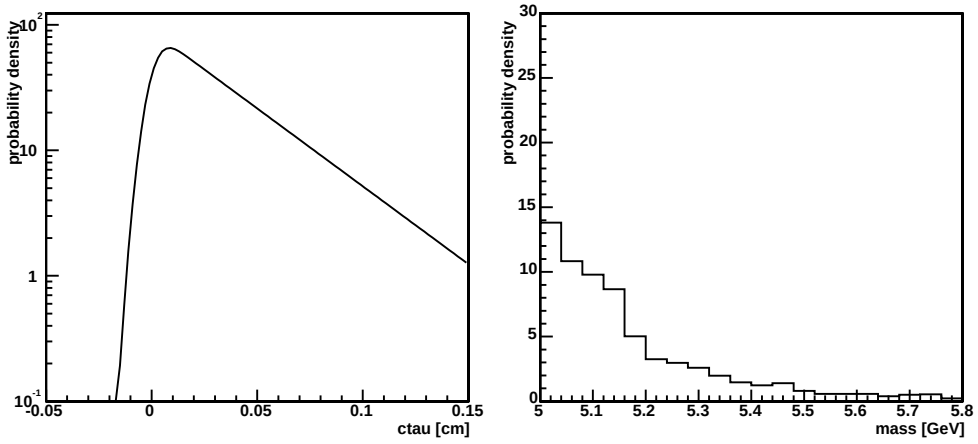

(a) Proper time PDF for the "missing decay products" contribution.

(b) Mass PDF for the "missing decay products" contribution.

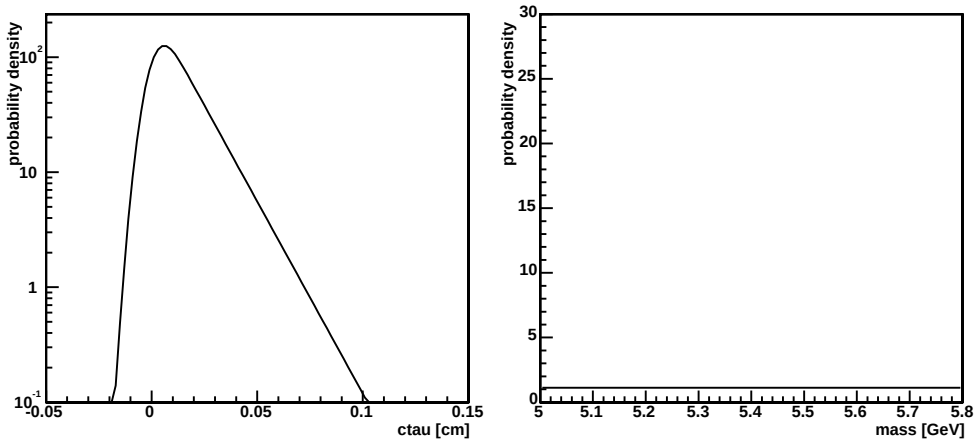

(c) Proper time PDF for the "unrelated K^0_S" contribution.

(d) Mass PDF for the "unrelated K^0_S" contribution.

FIG. 9: Probability density functions describing the two long-lived background contributions to our selected event sample.

- the $c\tau$ resolution scales $F_{c\tau,1}$ and $F_{c\tau,2}$, and α_2 which is the fraction of events following $F_{c\tau,2}$,
- the B^0_d lifetime $\lambda(B^0_d)$ and the time constants of the long-lived backgrounds $(c\tau)_{miss}$ and $(c\tau)_{unrel.K}$.

A. Fit results

We will begin by fixing the parameters that can be determined independently. By fitting a Gaussian plus an exponential (convoluted with a Gaussian) to the low-mass sideband data, we are able to obtain the shape of the prompt J/ψ $c\tau$ distribution, and a first indication of $(c\tau)_{miss}$. The fit result is given in Fig. 11 and Table III. To good approximation, the unrelated K^0_S contribution is the only long-lived contribution in the high-mass sideband. Therefore we can use the prompt J/ψ shape determined from the low-mass sideband, in combination with an exponential convoluted with a Gaussian, to fit for $(c\tau)_{unrel.K}$ in the high-mass sideband. Fig. 12 and Table IV show the results of this fit to the high-sideband data.

In our final two-dimensional fit, we set the resolution scales $F_{c\tau,1}$ and $F_{c\tau,2}$ to 1.65 and 5.49, and their relative weight α_2 to 0.05, as determined using the low-mass sideband data. We fix $(c\tau)_{unrel.K}$ to 173 μm. Fixing these

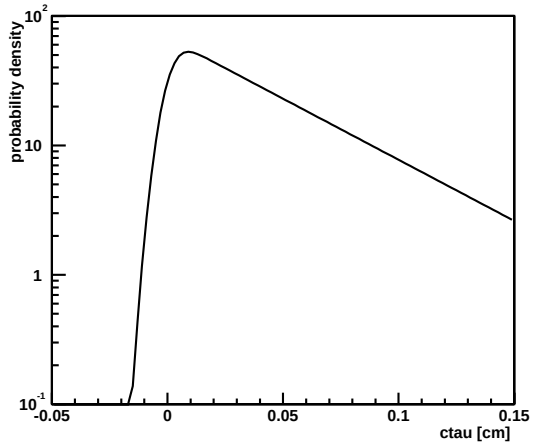

(a) Proper time PDF for signal.

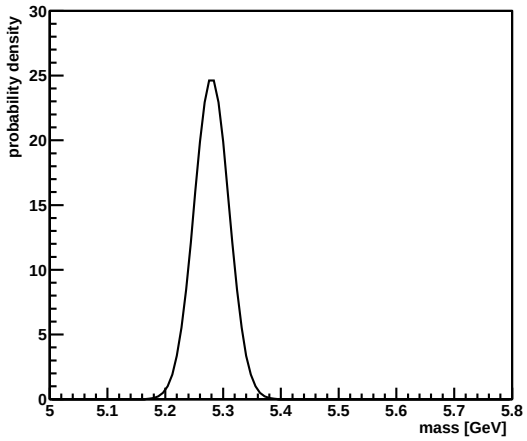

(b) Mass PDF for signal.

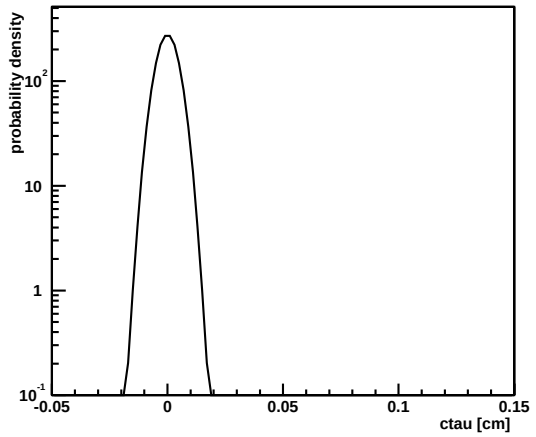

(c) Proper time PDF for prompt J/ψ contribution.

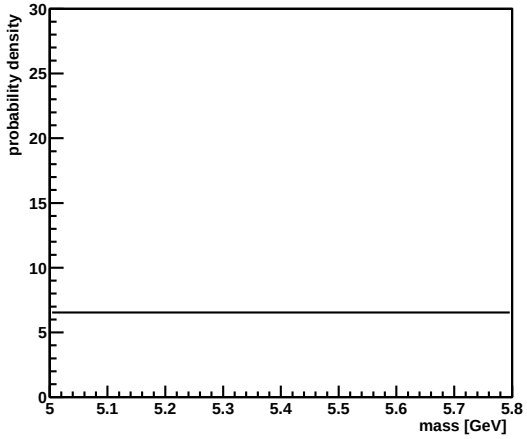

(d) Mass PDF for prompt J/ψ contribution.

FIG. 10: Shape of mass PDF's and proper time PDF's used for signal, and the background from prompt J/ψ's.

parameters leaves seven free parameters to be determined by the two-dimensional fit. The results are shown in Fig. 13 and Table V. The measured value of the B_d^0 lifetime is 468^{+95}_{-75} μm. The error has been determined by scanning the likelihood across a range of different values for the B_d^0 lifetime. A plot of the likelihood is shown in Fig. 14. The values of the B_d^0 lifetime that have a likelihood of 0.5 above the minimum are used to define the 1 σ confidence interval.

A total of 715 events falls within the mass and proper time window shown in the plots in Fig. 13. With the measured signal fraction of 0.054 ± 0.0161, this means we fit 39 ± 11.5 B_d^0's using this method. This number can be compared to the number of B_d^0's fitted in the mass distribution shown in Fig. 3 to the number found in the two-dimensional fit: 58 ± 20. The weighted average of the widths used to describe the B_d^0 peak in Fig. 13 is 40.4 MeV. This should be compared to the width of the peak in Fig. 3, which was 41 MeV. These numbers are consistent.

The lifetime plot in Fig. 13 makes it appear impossible to determine both exponential slopes. It should be realized however, that each slope is determined by a different mass region. This is confirmed by the correlation matrix of the fit:

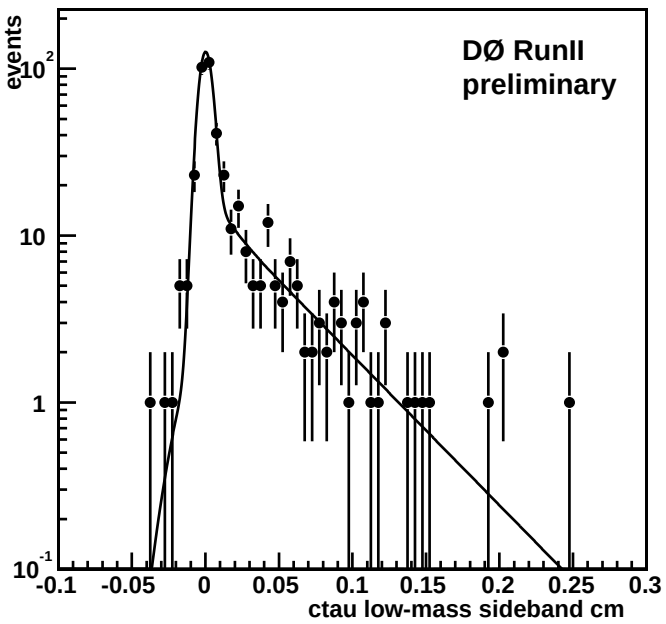

FIG. 11: A fit to the proper time distribution of events from the low-mass sideband (real data, mass range 4.1-5.1 GeV). The fit shape is a double Gaussian to fit the prompt J/ψ contribution and an exponential convoluted with a Gaussian to accommodate the long-lived background in this sample. The fit χ^2 per degree of freedom is 0.47.

Variable	value
lifetime $(c\tau)_{miss}$	483^{+46}_{-41} μm
prompt fraction α_{prompt}	0.66 ± 0.04
$c\tau$ resol. scale factor 1 $F_{c\tau,1}$	1.65 ± 0.150
$c\tau$ resol. scale factor 2 $F_{c\tau,2}$	5.49 ± 2.731
weight second scale α_2	0.05 ± 0.06

TABLE III: Results from fitting a double Gaussian and an exponential convoluted with a Gaussian to events from the low-mass sideband.

	α	$\sigma_{B,1}$	$\sigma_{B,2}$	$\alpha_{B,2}$	$\lambda(B^0_d)$	$c\tau_{miss}$	$\alpha_{unrel.K}$	α_{prompt}
α	1	0.0146	0.154	0.248	−0.306	−0.0115	−0.118	0.155
$\sigma_{B,1}$	0.0146	1	0.238	−0.412	−0.0148	0.00133	−0.00415	0.00188
$\sigma_{B,2}$	0.154	0.238	1	−0.405	−0.0547	−0.00683	−0.0261	0.0728
$\alpha_{B,2}$	0.248	−0.412	−0.405	1	−0.162	−0.00343	−0.0842	0.11
$\lambda(B^0_d)$	−0.306	−0.0148	−0.0547	−0.162	1	−0.0148	0.0805	−0.0764
$c\tau_{miss}$	−0.0115	0.00133	−0.00683	−0.00343	−0.0148	1	0.262	0.0322
$\alpha_{unrel.K}$	−0.118	−0.00415	−0.0261	−0.0842	0.0805	0.262	1	−0.328
α_{prompt}	0.155	0.00188	0.0728	0.11	−0.0764	0.0322	−0.328	1

No large correlations between the B^0_d lifetime and $(c\tau)_{miss}$ or $(c\tau)_{unrel.K}$ are observed.

VI. SYSTEMATIC UNCERTAINTIES

In this section we will study different effects that potentially affect the lifetime measurement. We will conclude with an estimate of the combined contribution of these effects to the uncertainty on our result.

A. Lifetime of the unrelated K^0_S contribution

The lifetime of the unrelated K^0_S contribution, $(c\tau)_{unrel.K}$, has been fixed in the fit producing our final result in Fig. 13. Therefore the uncertainty on this parameter adds to the systematic error of our result. We can investigate the effect of the uncertainty in two ways.

First, we can release $(c\tau)_{unrel.K}$, and let it be determined by the fit. The two-dimensional fit determines $(c\tau)_{unrel.K}$ to be 209 ± 57 μm, which agrees with our original measurement of 173^{+39}_{-30} μm (see Table IV). The measured B^0_d lifetime is 466^{+95}_{-75} μm, which is compatible with our original result.

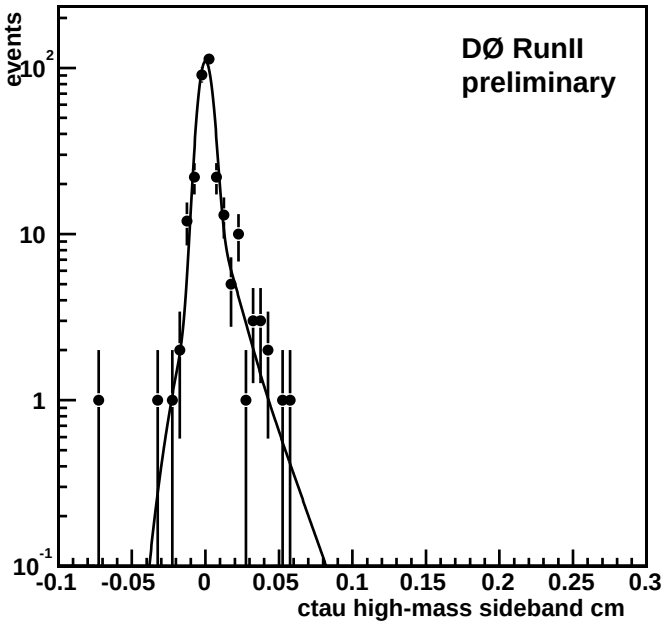

FIG. 12: A fit to the proper time distribution of events from the high-mass sideband (real data, mass range 5.6-6.6 GeV). The fit shape is a double Gaussian to describe the prompt J/ψ contribution and an exponential convoluted with a Gaussian to accommodate the long-lived background in this sample. The shape of the prompt J/ψ contribution has been fixed to the shape found in the high-mass sideband. The fit χ^2 per degree of freedom is 0.45.

Variable	value
lifetime $(c\tau)_{LL}$	173^{+39}_{-30} μm
prompt fraction α_{prompt}	0.88 ± 0.04
$c\tau$ resol. scale factor 1 $F_{c\tau,1}$	1.70 (fixed)
$c\tau$ resol. scale factor 2 $F_{c\tau,2}$	5.14 (fixed)
weight second scale α_2	0.10 (fixed)

TABLE IV: Results from fitting a double Gaussian and an exponential convoluted with a Gaussian to events from the high-mass sideband.

A second method of determining this uncertainty is by varying $(c\tau)_{unrel.K^0}$ with 1 σ, as it was determined in Fig. 12. The value was 173^{+39}_{-30} μm, so we set $(c\tau)_{unrel.K^0}$ to $(173 - 30)$ and $(173 + 39)$ and see how this affects our result. The fitted B^0_d lifetime is 468^{+94}_{-74} μm and 466^{+95}_{-75} μm respectively.

We assign a systematic error of 2 μm to this effect.

B. Long-lived background model

An incorrect model of the long-lived background may affect the lifetime measurement. We will therefore modify our background model and study the effect on our final result.

First we have adjusted the mass window for the two-dimensional fit to 5.1 - 6.5 GeV. According to our result in Fig. 13, only a very small contribution from the "missing decay products" event type will be left in our mass window. We therefore exclude this contribution from the fit by fixing $\alpha_{unrel.K}$ to 1. The result is shown in Fig. 15 and Table VI. The result is a B^0_d lifetime of 471^{+91}_{-70} μm, which is consistent with our official result of 468^{+95}_{-75} μm.

Another possible modification to our background model is to allow a slope in the mass distribution of the "unrelated K^0_S" contribution. One expects this mass distribution to fall toward higher masses, because relatively higher-p_T K^0_S's are needed, and the K^0_S p_T spectrum is a falling distribution. On the other hand, the slope is small when we determine it in a Monte Carlo sample of $B \to J/\psi X$ events. To allow a slope C in the mass distribution, we use the following normalized probability density function:

$$f^{mass}_{unrel.K} = \frac{1 + C \cdot (m_i - m_{min})}{(m_{max} - m_{min}) + C/2 \cdot (m_i - m_{min})^2} \tag{8}$$

Here m_{min} and m_{max} are the borders of the mass window, and m_i is the mass of the B^0_d candidate. For the slope of the "unrelated K^0_S" mass distribution C we find a value of 1.6 ± 7.1, which is consistent with zero. The B^0_d lifetime measurement measured this way is 454^{+89}_{-69} μm.

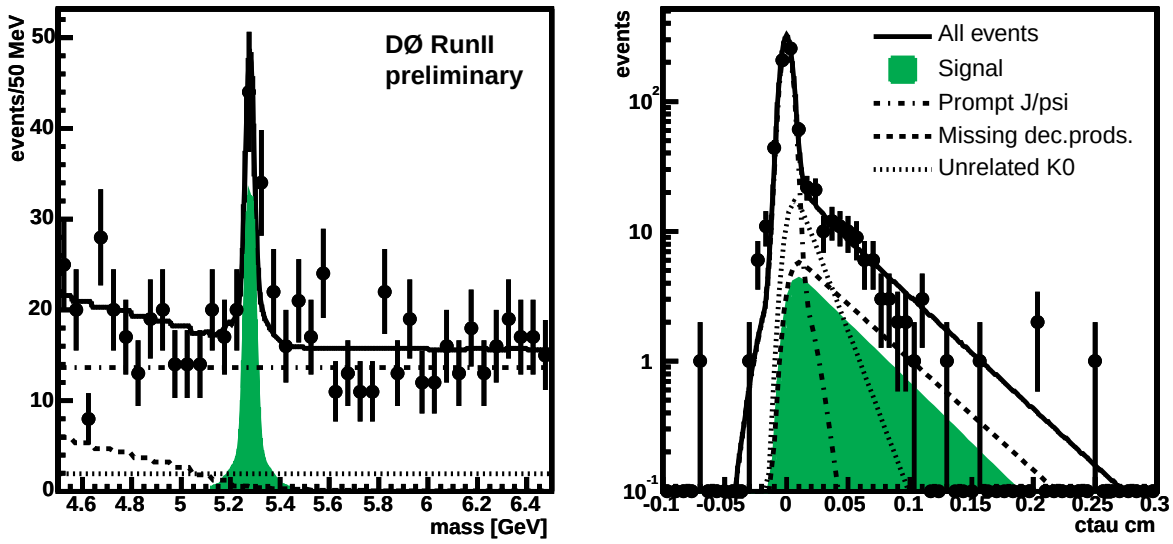

FIG. 13: Result from a two-dimensional fit, using mass and proper time information. The proper time shape of the prompt J/ψ contribution has been fixed, as well as the lifetime of the unrelated K^0_S contribution.

Variable	value
signal fraction α	0.054 ± 0.0161
$m(B^0_d)$	5.279 GeV (fixed)
B^0_d width 1	17.1 ± 6.02 MeV
B^0_d width 2	61.8 ± 34.22 MeV
$\alpha_{B,2}$	0.38 ± 0.288 MeV
$\lambda(B^0_d)$	468^{+95}_{-75} μm
lifetime $(c\tau)_{miss}$	510 ± 111 μm
fraction unrelated K^0_S's $\alpha_{unrel.K^0}$	0.58 ± 0.11
lifetime $(c\tau)_{unrel.K^0}$	173 μm (fixed)
prompt fraction α_{prompt}	0.81 ± 0.03
$c\tau$ resol. scale factor 1 $F_{c\tau,1}$	1.65 (fixed)
$c\tau$ resol. scale factor 2 $F_{c\tau,2}$	5.49 (fixed)
weight second scale α_2	0.05 (fixed)

TABLE V: Result from a two-dimensional fit, using mass and proper time information.

We now have three results from three different background models. We will assign the RMS of these three results as the systematic error due to uncertainty in our long-lived background model. The three results are 468 μm (official result), 471 μm (different mass range and no missing decay products) and 454 μm (slope in the unrelated K^0_S mass distribution). The RMS (given by $\sqrt{< x^2 > - < x >^2}$) of these three results is 7 μm. We therefore assign a systematic uncertainty of 7 μm to the possibility that our model of the long-lived background model is incorrect.

C. An additional unidentified background

It's possible that there is an additional background contribution that we have not identified yet. Perhaps it is difficult to conceive a background that is significant, but does not show up in any of the fits, but we can simply introduce it in the two-dimensional fit and see how our result is affected.

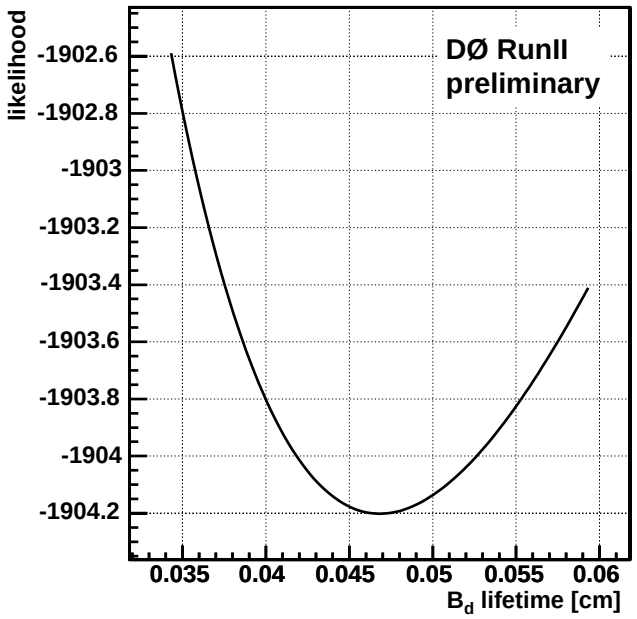

FIG. 14: The likelihood for different values of the B_d^0 lifetime.

We have implemented a background X, which we gave a normalization α_X, defined as a fraction of the "missing decay products" contribution. As a reminder, the current fractions are defined as follows: In the complete sample of selected events in a mass range from 4.5 to 6.5 GeV, we have signal and background, where the amount of signal is given by the signal fraction α. The background is split in prompt and long-lived, and the prompt contribution is normalized according to α_{prompt}. The long-lived contributions are divided in "unrelated K_S^0" and "missing decay products" (normalization given by $\alpha_{unrel.K}$). Now we split off a fraction α_X from the "missing decay products" contribution, and call that our unidentified contribution.

As a mass distribution, we use a uniform distribution, just as was used for the unrelated K_S^0's. As the proper time shape, we can use an exponential convoluted with a Gaussian. If we do this, the unidentified background has exactly the same characteristics as the unrelated K_S^0's, and the fit will give X a lifetime and normalization similar to the unrelated K_S^0's and a large correlation with the parameters of the unrelated K_S^0 contribution. We can also assume that our background is completely random in lifetime, i.e. that it has a uniform lifetime distribution. If we do this, we fit a normalization α_X of 0.2 ± 0.57 or 11 ± 32 events. This is consistent with zero events, and the B_d^0 lifetime is not affected: The result is 468^{+96}_{-74} μm.

D. Effects of the vertexing cuts

To study how the quality cuts that we make on the B_d^0 candidates affect the lifetime measurement, we have relaxed those cuts and fit B_d^0 lifetime in the resulting candidate sample. The cuts that affect vertex quality are the B_d^0 vertex χ^2, and perhaps also the number of SMT hits required on each track from the J/ψ. The optimal values of these cuts are 25 for the B_d^0 χ^2 and a minimum of 3 SMT hits. We have relaxed these to 100 and 1 respectively. While these cuts are non-optimal, they are still reasonable. The number of events increases from 715 to 770. The result of the two-dimensional lifetime fit is shown in Table VII. The B_d^0 lifetime measured using these modified cuts 448^{+87}_{-68} μm.

Part of the difference with the official result (20 μm) can be explained by statistical scatter, because there are more events in this fit, than were used for the official result. This statistical effect is difficult to quantify though, so we assign the entire effect of 20 μm as a systematic error.

E. Fitting strategy

We have begun fixing the prompt J/ψ proper time shape to the result from the low-mass sideband. We can also fit the prompt J/ψ proper time shape in the high-mass sideband and use this shape in the two-dimensional fit. This fit

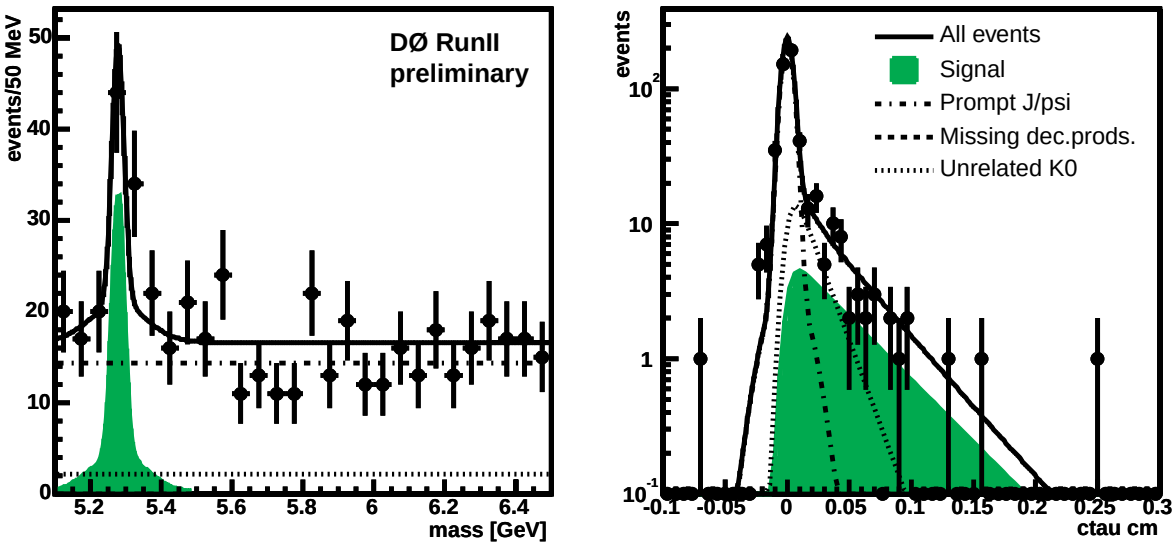

FIG. 15: Result from a two-dimensional fit, where we adjusted the mass window to 5.1-6.5 GeV and removed the "missing decay products" contribution from the fit.

Variable	value
signal fraction α	0.081 ± 0.0207
$m(B_d^0)$	5.279 ± 0.0000 GeV
B_d^0 width 1	17.2 ± 5.30 MeV
B_d^0 width 2	78.4 ± 75.34 MeV
$\alpha_{B,2}$	0.40 ± 0.200 MeV
$\lambda(B_d^0)$	471^{+91}_{-70} μm
slope C_{miss}	0.00 ± 0.00
lifetime $(c\tau)_{miss}$	370 ± 7 μm
fraction unrelated K_S^0's $\alpha_{unrel.K^0}$	1.00 ± 0.00
lifetime $(c\tau)_{unrel.K^0}$	173 ± 0 μm
prompt fraction α_{prompt}	0.87 ± 0.03
$c\tau$ resol. scale factor 1 $F_{c\tau,1}$	1.65 ± 0.000
$c\tau$ resol. scale factor 2 $F_{c\tau,2}$	5.49 ± 0.000
weight second scale α_2	0.05 ± 0.00

TABLE VI: Result from a two-dimensional fit, where we adjusted the mass window to 5.1-6.5 GeV and removed the "missing decay products" contribution from the fit.

will make one of the two Gaussians from the prompt J/ψ shape very wide, in order to include the single outlier at a $c\tau$ of -0.07 cm (see e.g. Fig. 12). The fit results for the proper time shape are $F_{c\tau,1} = 1.61 \pm 0.163$, $F_{c\tau,2} = 32 \pm 28$ and $\alpha_2 = 0.01 \pm 0.02$. The result for $(c\tau)_{unrel.K^0}$ is 124^{+26}_{-21} μm. If we use these values in the two-dimensional fit, we obtain the result shown in Fig. 17.

The result is 435^{+86}_{-70} μm, 33 μm below our final result. Therefore we assign a systematic uncertainty of 33 μm to this effect.

F. Bad muon runs

To verify that no adverse effects exist in the run range that was labeled "bad" by the muon group, but used in this analysis anyway, we exclude this data and refit the lifetime. The result for the B_d^0 lifetime becomes 472^{+112}_{-82} μm, so we conclude that there is no significant effect.

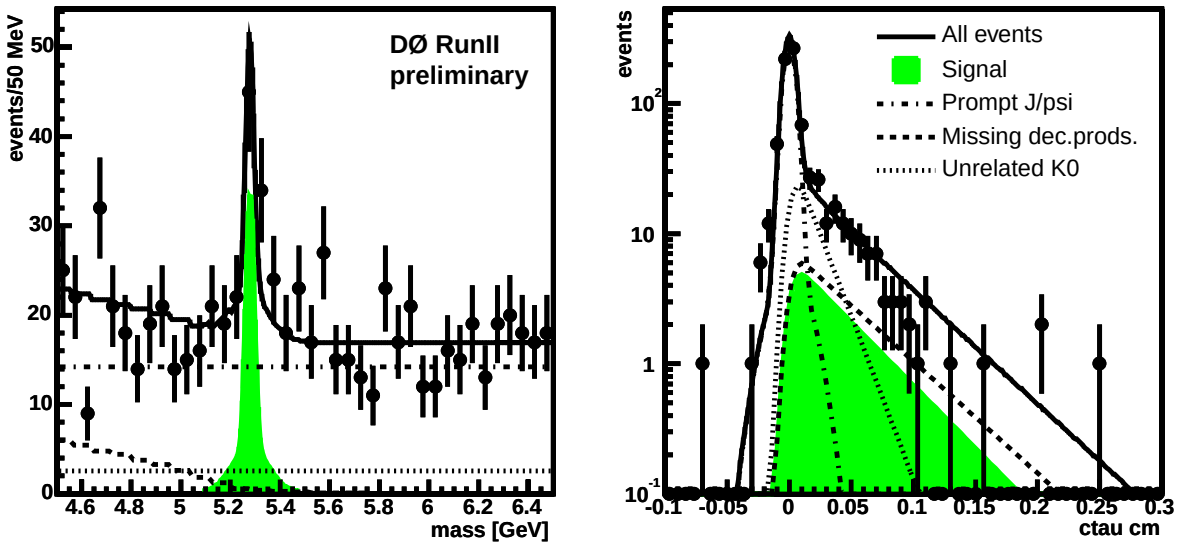

FIG. 16: Result from a two-dimensional fit, where we relaxed the cuts on the B_d^0 vertex χ^2 and the minimum number of SMT hits on the tracks from the J/ψ.

signal fraction α	0.055 ± 0.0169
$m(B_d^0)$	5.279 GeV (fixed)
B_d^0 width 1	16.9 ± 6.00 MeV
B_d^0 width 2	71.8 ± 32.52 MeV
$\alpha_{B,2}$	0.43 ± 0.264 MeV
$\lambda(B_d^0)$	448^{+87}_{-68} μm
lifetime $(c\tau)_{miss}$	505 ± 110 μm
fraction unrelated K_S^0's $\alpha_{unrel.K^0}$	0.65 ± 0.09
lifetime $(c\tau)_{unrel.K^0}$	173 μm (fixed)
prompt fraction α_{prompt}	0.78 ± 0.03
$c\tau$ resol. scale factor 1 $F_{c\tau,1}$	1.65 (fixed)
$c\tau$ resol. scale factor 2 $F_{c\tau,2}$	5.49 (fixed)
weight second scale α_2	0.05 (fixed)

TABLE VII: Result from a two-dimensional fit, using mass and proper time information. The cut on the B_d^0 vertex χ^2 had been relaxed to 100, and only a minimum of 1 SMT hit was required on each track from the J/ψ.

G. Summary of systematic effects

We have studied different possible effects on our B_d^0 lifetime measurement, and assigned the following uncertainties:

- Uncertainty on $(c\tau)_{unrel.K^0}$: 2 μm
- Long-lived background model: 7 μm
- Fitting strategy: 33 μm
- B_d^0 vertex quality cuts: 20 μm

Adding these uncertainties quadratically as independent effects yields an overall systematic error of 39 μm.

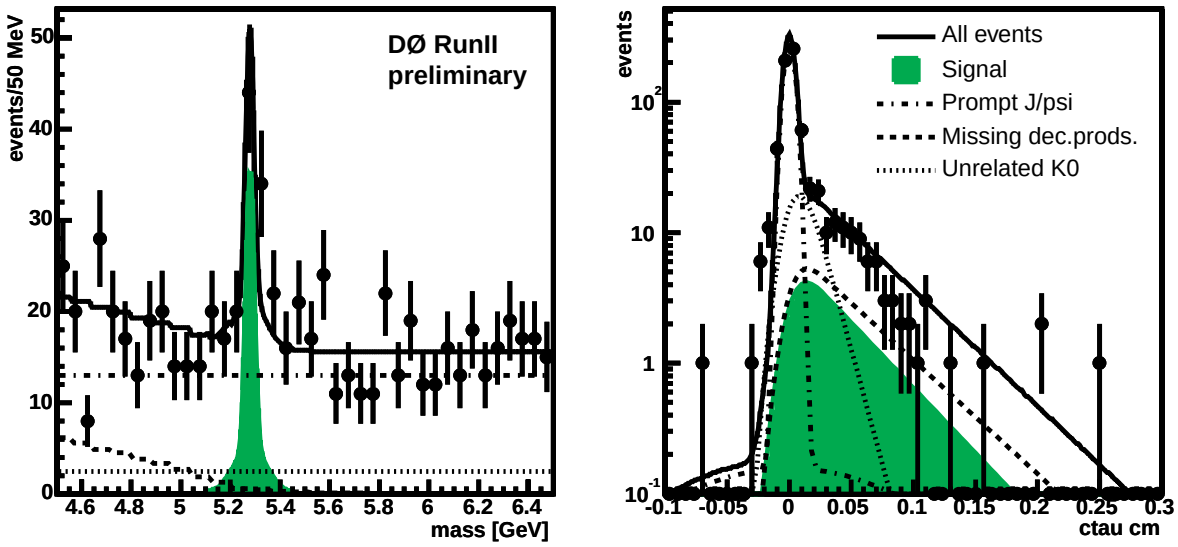

FIG. 17: Result from a two-dimensional fit, using mass and proper time information. The proper time shape of the prompt J/ψ contribution has been fixed, as well as the lifetime of the unrelated K^0_S contribution.

Variable	value
signal fraction α	0.057 ± 0.0171
$m(B^0_d)$	5.279 GeV (fixed)
B^0_d width 1	16.4 ± 5.61 MeV
B^0_d width 2	63.0 ± 32.53 MeV
$\alpha_{B,2}$	0.39 ± 0.276 MeV
$\lambda(B^0_d)$	435^{+86}_{-70} μm
lifetime $(c\tau)_{miss}$	498 ± 108 μm
fraction unrelated K^0_S's $\alpha_{unrel.K^0}$	0.63 ± 0.09
lifetime $(c\tau)_{unrel.K^0}$	124 μm (fixed)
prompt fraction α_{prompt}	0.77 ± 0.03
$c\tau$ resol. scale factor 1 $F_{c\tau,1}$	1.61 (fixed)
$c\tau$ resol. scale factor 2 $F_{c\tau,2}$	32.59 (fixed)
weight second scale α_2	0.01 (fixed)

TABLE VIII: Result from a two-dimensional fit, using an alternative fitting strategy.

VII. CONCLUSIONS

Using the DØ dimuon data, collected from October 2002 to June 2003, we have measured the B^0_d lifetime in the decay mode to J/ψ K^0_S to be $468^{+95}_{-75}(\text{stat.}) \pm 39(\text{syst.})$ μm, or:

$$\tau(B^0_d) = 1.56^{+0.32}_{-0.25}(\text{stat.}) \pm 0.13(\text{syst.}) \text{ ps}$$

This result is consistent with the current world average of 1.542 ± 0.016 ps [2].

VIII. ACKNOWLEDGEMENTS

We thank the staffs at Fermilab and collaborating institutions, and acknowledge support from the Department of Energy and National Science Foundation (USA), Commissariat à L'Energie Atomique and CNRS/Institut National de Physique Nucléaire et de Physique des Particules (France), Ministry for Science and Technology and Ministry for Atomic Energy (Russia), CAPES, CNPq and FAPERJ (Brazil), Departments of Atomic Energy and Science and Education (India), Colciencias (Colombia), CONACyT (Mexico), Ministry of Education and KOSEF (Korea), CONICET

and UBACyT (Argentina), The Foundation for Fundamental Research on Matter (The Netherlands), PPARC (United Kingdom), Ministry of Education (Czech Republic), Natural Sciences and Engineering Research Council and WestGrid Project (Canada), BMBF (Germany), A.P. Sloan Foundation, Civilian Research and Development Foundation, Research Corporation, Texas Advanced Research Program, and the Alexander von Humboldt Foundation.

---

[1] Information obtained from the Run Quality Database at `http://d0db.fnal.gov/qualitygrabber/qualQueries.html`
[2] Particle Data Group, *Review of Particle Physics*, Phys. Rev. D 66 (2002)
[3] A. Nomerotski, *Magnetic field in the DØ tracker volume*, DØ internal note 4312 (2003)